Biophysical Chemistry 265 (2020) 106434

Contents lists available at ScienceDirect

Biophysical Chemistry

journal homepage: www.elsevier.com/locate/biophyschem

Modulating Aβ aggregation by tyrosol-based ligands: The crucial role of the catechol moiety

Valeria Romanucci[a,1], Sara García-Viñuales[b,1], Carmelo Tempra[c,1], Roberta Bernini[d], Armando Zarrelli[a], Fabio Lolicato[e,f,*], Danilo Milardi[b,**], Giovanni Di Fabio[a,**]

[a] Department of Chemical Sciences, University of Naples Federico II, Via Cintia 4, I-80126 Napoli, Italy
[b] Consiglio Nazionale delle Ricerche Istituto di Cristallografia, Via Paolo Gaifami 18, 95126 Catania, Italy
[c] Institute of Organic Chemistry and Biochemistry of the Czech Academy of Sciences, Flemingovonám. 542/2, CZ-16610 Prague, Czech Republic
[d] Department of Agriculture and Forest Science (DAFNE), University of Tuscia, Via S. Camillo De Lellis, 01100 Viterbo, Italy
[e] Heidelberg University Biochemistry Center, Im Neuenheimer Feld 328, 69120 Heidelberg, Germany
[f] Department of Physics, University of Helsinki, P.O. Box 64, FI-00014 Helsinki, Finland

HIGHLIGHTS

- 3-hydroxytyrosol (HDT) is an effective potent inhibitor of Aβ amyloid growth.
- Tyrosol (TY), and 3-methoxytyrosol (homovanillyl alcohol - HVA) do exhibit an opposite effect and catalyze Aβ aggregation.
- Molecular dynamics simulations reveal an H-bond network that bridges HDT, but not TY and HVA, with the G22 residue of Aβ.

GRAPHICAL ABSTRACT

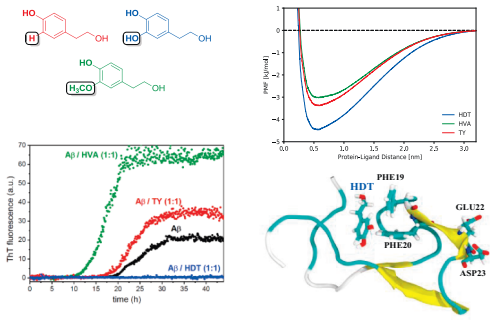

ARTICLE INFO

Keywords:
Alzheimer's disease
Aβ anti-aggregation
Tyrosol
Hydroxytyrosol
Homovanillyl alcohol

ABSTRACT

The abnormal deposition of Aβ amyloid deposits in the brain is a hallmark of Alzheimer's disease (AD). Based on this evidence, many current therapeutic approaches focus on the development of small molecules halting Aβ aggregation. However, due to the temporary and elusive structures of amyloid assemblies, the rational design of aggregation inhibitors remains a challenging task. Here we combine ThT assays and MD simulations to study Aβ aggregation in the presence of the natural compounds tyrosol (TY), 3-hydroxytyrosol (HDT), and 3-methoxytyrosol (homovanillyl alcohol - HVA). We show that albeit HDT is a potent inhibitor of amyloid growth, TY and HVA catalyze fibril formation. An inspection of MD simulations trajectories revealed that the different effects of these three molecules on $A\beta_{1-40}$ aggregation are ascribable to their capacity to arrange H-bonds network between the ligand (position C-3) and the peptide (Glu22). We believe that our results may contribute to the design of more effective and safe small molecules able to contrast pathogenic amyloid aggregation

Abbreviations: Aβ, Amyloid-beta; AD, Alzheimer's disease; ThT, Thioflavin T; TY, tyrosol; HDT, 3-hydroxytyrosol; HVA, 3-methoxytyrosol; EVOO, extra-virgin olive oil; MD, molecular dynamics; PMF, potential of mean force; RMS, root mean square; RMSD, root mean square deviation; RMSF, root mean square fluctuation

* Corresponding author at: Heidelberg University Biochemistry Center, Im Neuenheimer Feld 328, 69120 Heidelberg, Germany.
** Corresponding authors.
E-mail addresses: Fabio.lolicato@bzh.uni-heidelberg.de (F. Lolicato), danilo.milardi@cnr.it (D. Milardi), difabio@unina.it (G. Di Fabio).
[1] These authors contributed equally.

https://doi.org/10.1016/j.bpc.2020.106434
Received 7 April 2020; Received in revised form 30 June 2020; Accepted 12 July 2020
Available online 17 July 2020
0301-4622/

1. Introduction

Alzheimer's disease, the most common type of dementia, is a devastating neurodegenerative disease characterized by progressive neurocognitive dysfunction [1]. Alzheimer's a multifaceted disease for which several factors, such as cholinergic dysfunction, accumulation of amyloid-β (Aβ), and tau (τ)-protein as well as reduced blood supply in the brain, have been supposed to be relevant for its development [2]. Massive deposition of amyloid fibers in the brain is preceded by the accumulation of β-sheet-rich soluble Aβ oligomers or pre-fibrillar intermediates, that represent the most toxic agents in AD. Amyloid plaques are mainly composed of an excess of 40- and 42-mer amyloid β-proteins ($A\beta_{1-40}$ and $A\beta_{1-42}$), which are produced from the abnormal cleavage of amyloid precursor protein (APP) by β- and γ-secretases in a 9:1 M ratio $A\beta_{1-40}/A\beta_{1-42}$.

While $A\beta_{1-42}$ is more prone to form toxic aggregates, $A\beta_{1-40}$ is more abundant and soluble, and for this reason, it represents an ideal substrate for many biophysical studies [3]. Furthermore, NMR studies focusing on the interactions of the amyloid peptide with oleuropein, a natural compound with a catechol moiety, evidenced that only the central part of the peptide Glu11-Lys28 exhibits the most crucial proton resonance shifts thus confirming that $A\beta_{1-40}$ do provide a reliable picture of amyloid-ligand binding modes [4]. Accumulating evidence suggests that Aβ soluble oligomers are the most toxic amyloid species, which insert in cellular membranes creating pores and deregulating Ca^{2+} homeostasis [5]. However, mature fibrils are not devoid of cytotoxicity: amyloid fibrils interact with the lipidic bilayer surface and induce the thinning and disruption of the cell membrane through a detergent-like mechanism [6]. Besides their intrinsic toxicity, amyloid fibrils are also able to catalyze the formation of toxic oligomeric species through a secondary nucleation process and generate oxidative stress and inflammation [7–9]. Imaging studies have shown that plaques could start to form 10–15 years before symptoms emerge, prompting researchers to consider amyloid-β the first target for AD prevention [10]. That is why a current strategy to prevent AD includes the design of new molecules able to inhibit the self-assembly of Aβ [11].

Many reports have described the active role of small molecules based on natural polyphenols in the development of AD therapeutic agents that specifically and efficiently get involved in different stages of the aggregation process, preventing the formation of fibrillar Aβ aggregates. Several dietary polyphenols such as epigallocatechin-3-gallate, curcumin, resveratrol, ferulic acid, silybin B [12,13], and myricetin have shown a disrupting effect on Aβ aggregation, and some of them are currently under clinical trials for AD treatment [14]. On the other hand, a rational drug design of small molecules capable of targeting Aβ and modulating its aggregation pathway remains a challenging task in the development of AD therapies.

In this frame, natural polyphenols that exhibit anti-amyloid effects have distinct advantages over other synthetic compounds; in fact, they are often daily consumed as part of a healthy diet and offer known nutraceutical benefits thanks to their several promising pharmacological properties including antioxidant, anti-inflammatory, anti-cancer, and anti-atherosclerosis effects. Recently, polyphenols found into extra-virgin olive oil (EVOO), a vital component of the Mediterranean diet, have attracted considerable interest [15–17]. In particular, three polyphenols contained in EVOO, i.e., 3-hydroxytyrosol (HDT), oleuropein (OLE), and tyrosol (TY) deserve special consideration. Indeed, while many of their possible pharmacological uses have been extensively investigated [18], only recently, they have been studied as anti-AD agents [19,20]. In vitro studies have revealed that HDT interferes with the path of amyloid aggregation of some peptides/proteins, including $A\beta_{1-42}$ and tau (τ) protein, offering protection against amyloid β-induced neurotoxicity in different neuronal cell lines [21,22]. Recently Leri et al. have reported that HDT inhibits the formation of ThT-positives $A\beta_{1-42}$ fibrils [21]. However, a quantitative estimate of the effects of HDT on aggregation kinetics is still unavailable.

Furthermore, comparative studies conducted on different natural HDT conjugated (Acteoside, phenyl ethanoid glycosides, Verbascoside, Rutin) [23,24], have shown that inhibition of Aβ amyloid aggregation could be mainly attributed to the catechol moiety. However, the mechanisms making the catechol moiety a critical molecular factor in driving ligand-amyloid interactions are unknown.

In this work, we address this question by performing ThT aggregation assays on three slightly different polyphenols: tyrosol (TY), 3-hydroxytyrosol (HDT), and 3-methoxytyrosol (homovanillyl alcohol - HVA). The considerable differences exhibited by the three ligands in affecting $A\beta_{1-40}$ aggregation kinetics are discussed in the light of ligand/peptide molecular dynamics simulations.

2. Materials and methods

2.1. Chemicals

Tyrosol (TY) and 3-methoxytyrosol (HVA) were purchased from Sigma Aldrich, while 3-hydroxytyrosol (HDT) was synthesized according to reported in the literature [25]. Synthetic amyloid beta-peptide ($A\beta_{1-40}$) was purchased from GenScript. Thioflavin T (ThT) was purchased from Sigma Aldrich. Unless otherwise specified, all chemicals (analytical grade) were purchased from Carlo Erba. All solutions were prepared with ultrapure Thermo Milli Q water.

2.2. Monomerization of $A\beta_{1-40}$

Stock solutions of $A\beta_{1-40}$ were prepared by solubilizing the peptide in HFIP (1 mg/mL). Small aliquots (100 μL) of the stock solutions were frozen at −80 °C and lyophilized. Quantification of Aβ aliquots was performed by dissolving the lyophilized protein powder in 20 μL of NaOH 1 mM, adding it to 180 μL of buffer (phosphate 10 mM, pH 7.4) and measuring the absorbance at 280 nm (ε_{280} = 1450 M^{-1} cm^{-1}). The monomeric state of freshly prepared $A\beta_{1-40}$ solutions was routinely confirmed by western blot analysis as elsewhere reported [13].

2.3. ThT assays

Samples were prepared by adding 1–2 μL of 1–10 mM HDT, HVA or TY stock solutions in DMSO (final ligand concentrations 5 μM, 10 μM or 20 μM; final DMSO concentration was maintained at 2%) to 50 μL of ThT 20 μM in buffer (phosphate 10 mM, pH 7.4, NaCl 100 mM). Experiments were carried out in 384-well plates. Immediately after addition of $A\beta_{1-40}$ (20 μM, final concentration), time traces were recorded using a Varioskan plate reader (ThermoFisher, Waltham, MA) with λ_{exc} 440 nm and λ_{em} 480 nm at 37 °C. The plate was shaken for 10 s before each read (600 shakes per minute with a diameter of the orbital movement of 1 mm). Controls in presence and absence of 2%

Table 1
Simulations details.

Protein (#)	Ligand (#)	# Water	# Na	# Cl	Time (ns)	# Replica
$A\beta_{1-40}$ (1)	(0)	8734	19	16	1000	1
$A\beta_{1-40}$ (1)	HDT (1)	10,815	24	21	100	100
$A\beta_{1-40}$ (1)	HVA (1)	10,815	24	21	100	100
$A\beta_{1-40}$ (1)	TY (1)	10,818	24	21	100	100

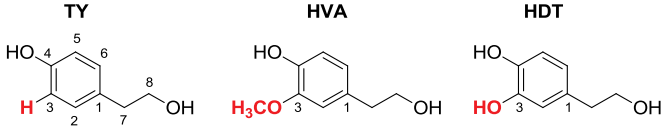

Fig. 1. Tyrosol ligands under investigation: tyrosol (TY), 3-methoxytyrosol (HVA), and 3-hydroxytyrosol (HDT).

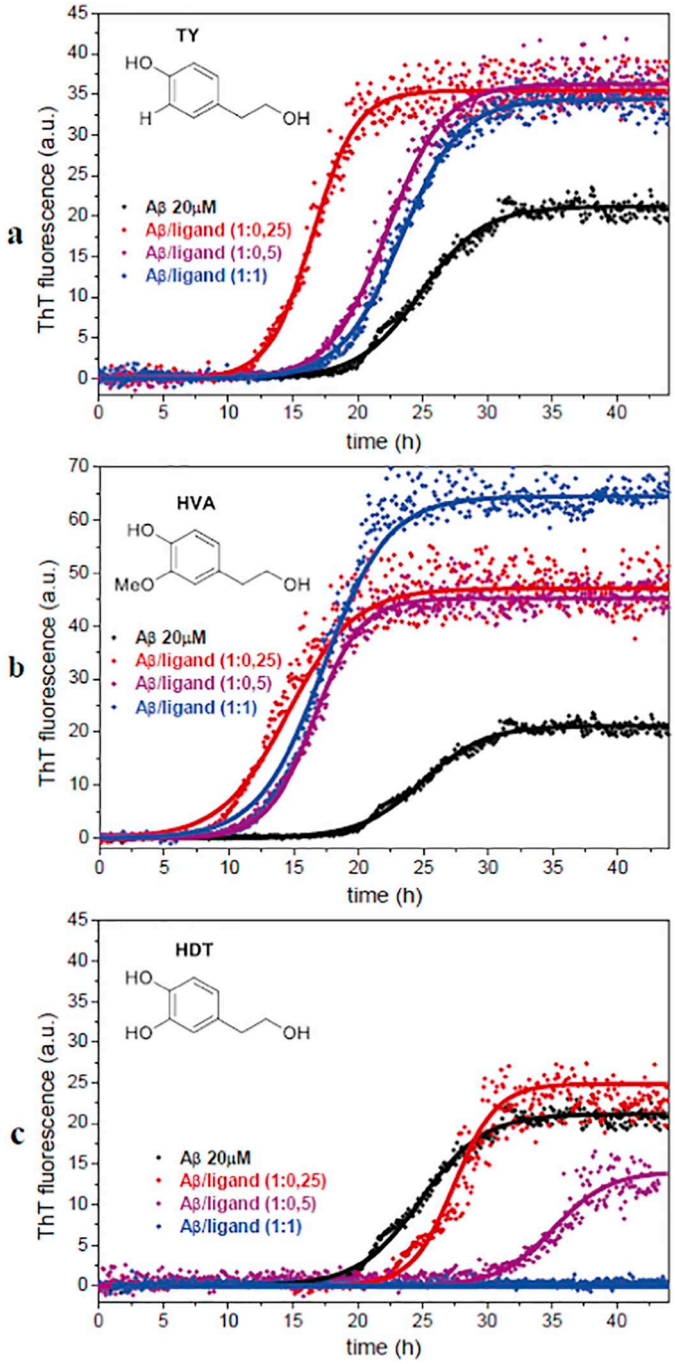

Fig. 2. Aggregation kinetics of $A\beta_{1-40}$ (20 μM) in the presence of TY (**a**), HVA (**b**), and HDT (**c**) compounds. Dots represent experimental data; the continuous line is the fit of the kinetic curves.

DMSO were carried out to exclude possible changes in $A\beta_{1-40}$ aggregation kinetics due to its presence. Controls in the absence of $A\beta_{1-40}$ were also performed for each tested condition to exclude false ThT positive signals unrelated to amyloid. Each experiment was performed in triplicate, and the characteristic parameters of $A\beta_{1-40}$ aggregation were obtained by fitting each kinetic curve with the following equation:

$$I = \frac{I_{max}}{1 + e^{-[k\cdot(t-t_{1/2})]}}$$

Were I is the fluorescence intensity as a function of time t, I_{max} represents the maximum intensity of fluorescence, k is the apparent rate constant, $t_{1/2}$ corresponds with the point in time where the signal reaches 50% of the amplitude of the transition; lag time (t_{lag}) has been defined as $t_{1/2} - 2/k$. Data are expressed as the average of the kinetic parameter obtained by fitting each of the replicas and indicated as mean (standard deviation) [26].

2.4. Molecular dynamics simulations

For atomistic molecular dynamics (MD) simulations, we employed GROMACS 2019 package [27]. We used a previously equilibrated [13] 3D structure of $A\beta_{1-40}$ (PDB ID: 2LFM [28]), which was further stimulated in water for 1 microsecond using the improved force field CHARMM36m [29] for intrinsically disordered proteins. Compared to the original deposited structure in the PDB database (which has a partial alpha helix), the used structure has a beta-hairpin (see Fig. S2 for the secondary structure information).

Water and ions particles were treated with CHARMM TIP3P water model and the standard CHARMM36 ions model, respectively. To solve the equations of motion, we used the Leap-Frog integrator with a 2 fs time step. Long-range electrostatic interactions were explicitly calculated employing Particle Mesh Ewald [30] (PME) algorithm with a cut-off length of 1.2 nm. Short-range interactions were, instead, treated applying a force-switching algorithm and a cut-off of 1.2 nm. Nose-Hoover [31] thermostat and Parrinello-Rahman [32] barostat were used to keep constant temperature and pressure, respectively. The temperature was kept at 310 K with a time constant of 1.0 ps, whereas the pressure was maintained at 1 bar with a time constant of 5.0 ps.

Protein and ligand (peptide/ligand ratio of 1:1) were first placed at a non-interacting distance of about 2 nm, and the simulation time was set to 100 ns for each of the one hundred independent replicas. The one hundred independent configurations were generated by randomly positioning the ligands around the $A\beta_{1-40}$ peptide. The systems were neutralized by an appropriate number of sodium and chloride atoms. NaCl salt at a concentration of 100 mM was added to mimic experimental conditions.

Detailed information about the simulation can be founded in Table 1. The first 50 ns of each simulation were discarded and considered as equilibration time. The last 50 ns were, instead, concatenated together to make a single trajectory from which we characterized the protein-ligand binding. The PMF was computed from the radial distribution function (RDF, $g(x)$) using the following equation: PMF = -RTln(g(x)). The initial structure, together with all the files needed to

Table 2
Sigmoidal fit equation and characteristic parameters of $A\beta_{1-40}$ aggregation kinetics in the presence of TY, HVA, and HDT in different peptide/ligand ratios.

	I_{msx} (*u. a.*)	k (h^{-1})	$t_{1/2}$ (h)	t_{lag}(h)
Aβ	21.2 (6.4)	0.41 (0.06)	24.9 (3.9)	20.1 (4.4)
Aβ/TY (1:0.25)	35.5 (13.1)	0.59 (0.07)	16.5 (3.8)	13.1 (3.8)
Aβ/TY (1:0.5)	36.2 (6.6)	0.45 (0.01)	22.3 (2.6)	17.8 (2.5)
Aβ/TY (1:1)	34.4 (8.6)	0.43 (0.01)	23.3 (2.6)	19.6 (1.0)
Aβ/HVA (1:0.25)	47.1 (14.8)	0.39 (0.11)	14.5 (2.0)	8.7 (3.3)
Aβ/HVA (1:0.5)	45.2 (9.2)	0.55 (0.04)	16.6 (0.6)	13.3 (5.4)
Aβ/HVA (1:1)	64.4 (25.9)	0.40 (0.16)	17.3 (5.6)	11.56 (8.5)
Aβ/HDT (1:0.25)	24.9 (14.1)	0.61 (0.28)	27.4 (14.0)	30.2 (12.2)
Aβ/HDT (1:0.5)	14.05 (11.1)	0.47 (0.02)	35.1 (8.8)	35.7 (4.7)
Aβ/HDT (1:1)	No aggregation	No aggregation	No aggregation	No aggregation

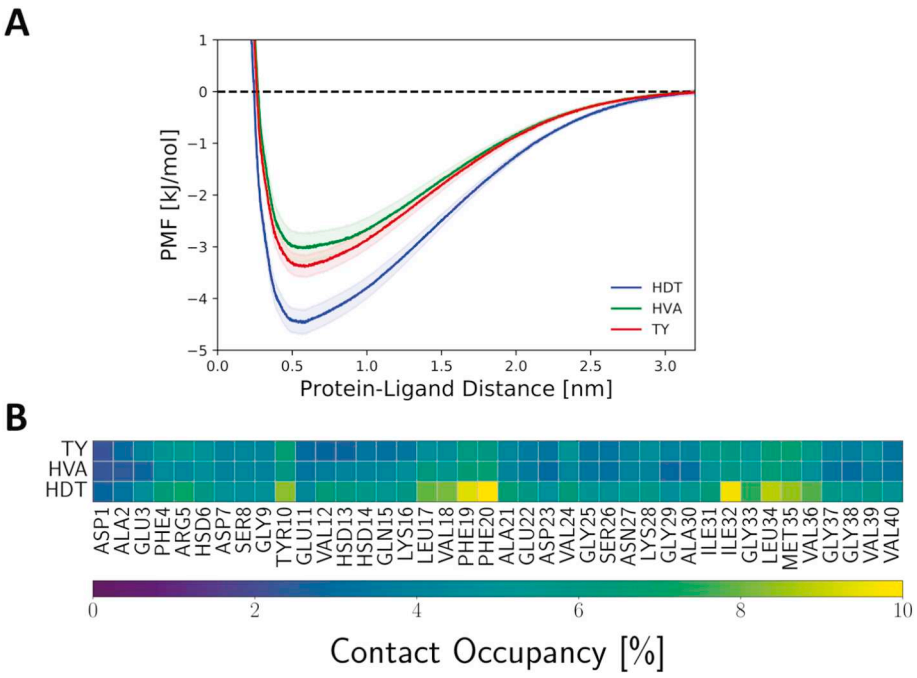

Fig. 3. A) Free energy profile of the protein-ligand binding as a function of their distance. The standard errors are shown as shadows.; B) Residue contact occupancy map. A contact is being calculated when the distance between two atoms is less than 0.6 nm.

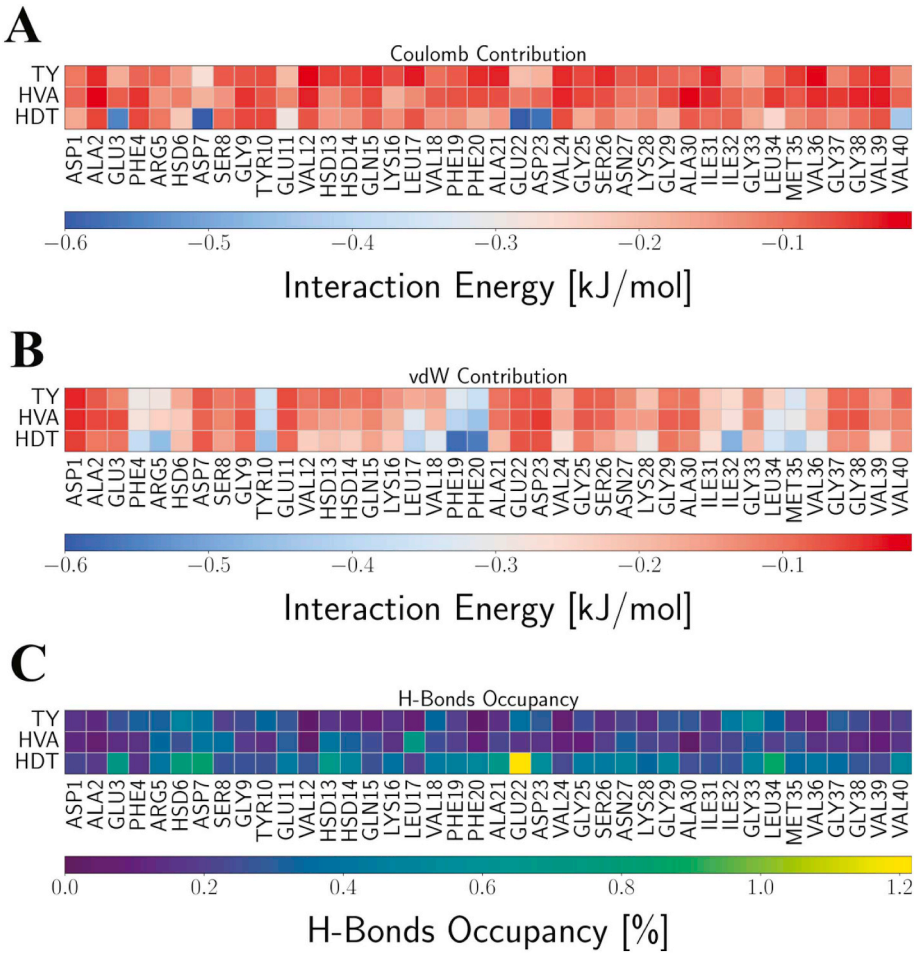

Fig. 4. Characterization of the protein-ligand binding. Panel A and B show the long and short-range interaction maps, respectively. Panel C shows the hydrogen bond occupancy between the residues of $A\beta_{1-40}$ and HDT, HVA, TY ligands. The respective bar plots of the maps are reported in Fig. S3–6.

run the simulations, as well as the trajectories and all the RAW files of the analysis, are publicly available at the following link: doi:https://doi.org/10.5281/zenodo.3908526.

3. Results and discussion

We first investigated by ThT assay the ability of tyrosol (TY), 3-methoxytyrosol (HVA) and 3-hydroxytyrosol (HDT) [25] to interfere with $A\beta_{1-40}$ aggregation.

Their anti-amyloidogenic behaviors have been analyzed depending on specific chemical structure variations; in particular, it has been examined how the presence of hydrogen/methoxy/hydroxyl (TY/HVA/HDT) at the C-3 position (Fig. 1) could influence ligand binding with $A\beta_{1-40}$ amyloid.

First, we monitored $A\beta_{1-40}$ (20 μM) fibril growth in the presence of different peptide/ligand molar ratios (1:0.25, 1:0.5, and 1:1). ThT is a highly specific probe of amyloid fibrils, increasing its fluorescence upon binding to β-rich structures, as amyloid fibrils, and presenting no changes of fluorescence in the presence of other kind of structures as monomers, oligomers or amorphous aggregates. Thus, the differences in the obtained $A\beta_{1-40}$ aggregation kinetic curves in the presence of different ligands could be attributed to different abilities in modulating $A\beta_{1-40}$ aggregation, as is the case of TY, HDT and HVA (Fig. 2). It is known that poorly soluble small ligands may inhibit amyloid growth via non-specific colloidal interactions occurring at high ligand/peptide molar ratios [33]. However, the experimental conditions adopted in aggregation assays, the significantly different effects taking place even in the lag phase of fibril formation, and the solubility of the three compounds in water [34], support the hypothesis that they bind peptide monomers by specific ligand-monomer interactions. The characteristic parameters of $A\beta_{1-40}$ aggregation kinetics in the presence of different tyrosols in different peptide/ligand ratios are reported in Table 2. In particular, TY accelerated the formation of ThT-positive fibrils compared with $A\beta_{1-40}$ aggregation in the absence of ligand, showing a decrease in the lag phase of approximately 7 h when a peptide/ligand molar ratio 1:0.25 was used (Table 2).

However, lag phase reduction was less evident by increasing the peptide/ligand molar ratio, i.e., the acceleration of $A\beta_{1-40}$ aggregation in the presence of TY resulted inversely related to the dose. Independently from the used peptide/ligand ratio, the maximum ThT fluorescence was increased by 75% compared to the aggregation kinetics in the absence of ligands suggesting, at least qualitatively, an increase in the amount of ThT-positive fibrils (Fig. 2a). HVA catalyzed the $A\beta_{1-40}$ aggregation showing a lag phase of 9–13 h in all the assayed peptide/ligand ratios (1:0.25, 1:0.5 and 1:1). The plateau of the curve was also increased in the presence of HVA, with a maximum effect observed at 1:1 M ratio (Fig. 2b).

However, HDT showed a different behavior, inhibiting the formation of ThT-positive fibrils. Submolar amounts of ligand produced an increase in the lag phase, and in the presence of equimolar amounts, the aggregation did not take place (Fig. 2c).

Our results are in accordance with literature data reporting an inhibitory effect of HDT and, what is more, highlight a different mechanism of the three molecules in modulating $A\beta_{1-40}$ aggregation.

To shed light on the molecular details of the interaction between $A\beta_{1-40}$ and the three ligands, we employed molecular dynamics simulations. For each of them, we carried out one hundred independent simulations 100 ns long with a peptide/ligand ratio of 1:1 (Table 2). All simulations have been concatenated together to make a single trajectory from which we characterized the protein-ligand binding. The potential of mean force (PMF) profile of the protein-ligand binding showed in Fig. 3 (panel A) sharpens the binding with $A\beta_{1-40}$ is thermodynamically favorable for all three metabolites ($\Delta G < 0$). While HVA and TY–protein complexes are sharing a free energy minimum at ~2.5 kJ/mol (the probability of finding the complex is 50% compared with the likelihood of finding the molecules dissociated). $A\beta_{1-40}$ - HDT complex, instead, exhibits higher stability with a minimum of ~4 kJ/mol, which means the formation of the complex is five times more likely than seeing the two molecules apart. The contact maps in Fig. 3 (panel B), indeed, show that none of the three metabolites a specific binding site, but rather, there are multiple binding motifs (the maximum contact occupancy value for the same amino acid is 10% only). The contact maps, however, show us another critical aspect. Although all of them seem interacting with the same residue patterns, HDT has a higher probability of interacting with the amino acid portion 16–19

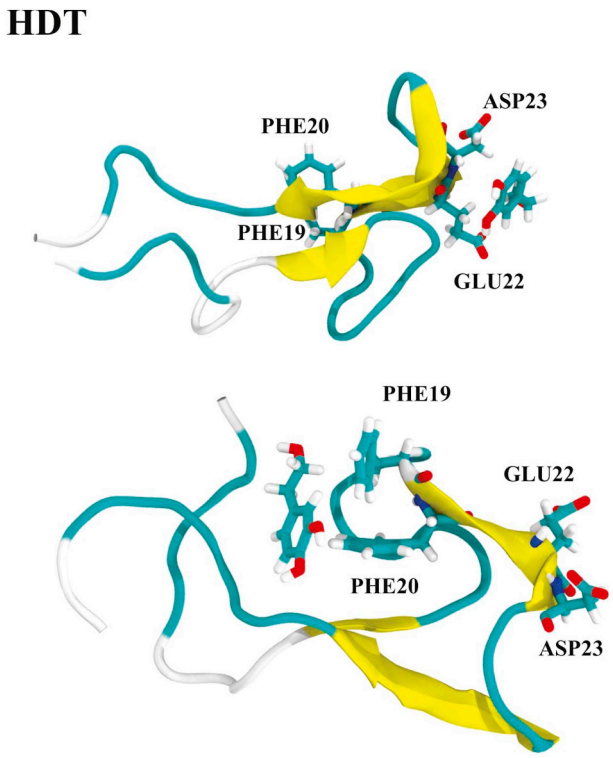

Fig. 5. Snapshots of the $A\beta_{1-40}$ -HDT complexes. The hydroxyl group forms multiple hydrogen bonds with residue GLU 22 (upper panel), which further allows pi-stacking interactions with residues PHE 19 and 20 (bottom panel).

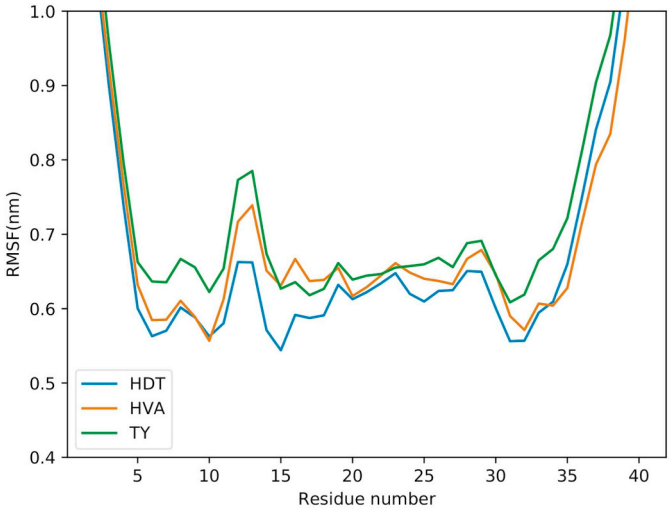

Fig. 6. The root-mean-square fluctuation (RMSF) per residue. The RMSF was calculated by best-fitting the backbone heavy atoms of each snapshot to the average structure. The RMSF is averaged from 100 MD simulations. Blue, orange, and green indicate the systems with HDT, HVA, and TY, respectively. (For interpretation of the references to colour in this figure legend, the reader is referred to the web version of this article.)

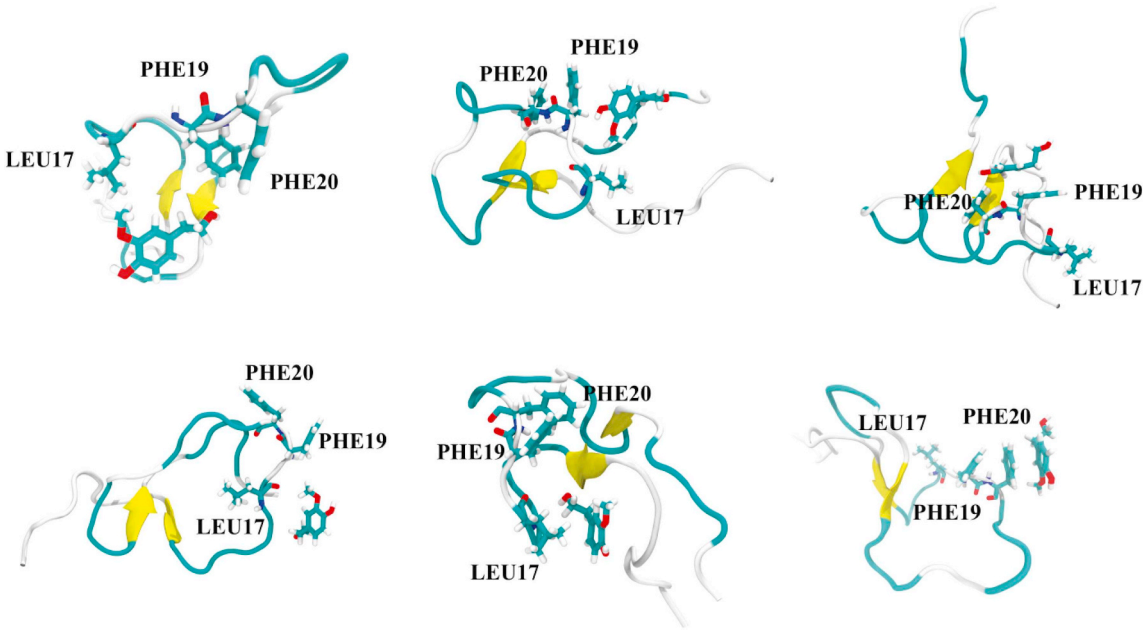

Fig. 7. Snapshots of the $A\beta_{1-40}$-HVA complexes highlighting hydrogen bonds formation between $A\beta_{1-40}$ and LEU 17, which can further drive it to pi-stacking with the PHE 19 and 20.

(and 31–35), which is known to be responsible for amyloidogenic aggregation [35]. This is in agreement with the ThT experiments showed in Fig. 2, and it would explain why HDT is the only one capable of inhibiting the formation of ThT-positive fibrils by blocking the 16–19 amino acidic portion of $A\beta_{1-40}$. Furthermore, the analysis of the interaction energies and hydrogen bond occupancy (Fig. 4) suggests the presence of the hydroxyl group in HDT on the C-3 position, plays a crucial role in stabilizing the interaction with $A\beta_{1-40}$. Indeed the hydroxyl group might serve as the first recruitment motif: it is capable of forming multiple hydrogen bonds with residue GLU 22 (Fig. 5 for cartoon representations), which further can allow pi-stacking interactions (see van der Waals energies in Fig. 4B) with residues PHE 19 and 20. Finally, we suggest that the stronger binding between HDT and $A\beta_{1-40}$ blocks the known amylogenic motif by stiffening the16–19 region of the protein and, then, prevents protein on-pathway aggregation.

The RMSF graph confirms the reduction in protein flexibility in Fig. 6: The RMSD of the 16–19 region has an average value of 0.6 nm, especially if compared to the cases where $A\beta_{1-40}$ interacts with HVA and TY (higher flexibility). The flexibility of this amino acid segment might be responsible for protein aggregation, as it also suggested in recent literature [36,37].

Based on the ThT assays, both HVA and TY catalyze fibril formation (Fig. 2). However, HVA accelerates fibril formation by showing a decrease in the lag phase of approximately 10 h already at a 1:1 protein/ligand ratio.

The structural difference between the two compounds is only the methyl ether at position 3, which allows hydrogen bonds formation with LEU 17 (Figs. 6, 7), which can further drive it to pi-stacking with the PHE 19 and 20. Furthermore, the interaction with HVA is the sole to increase the flexibility of the region 19–25 of the $A\beta_{1-40}$, which might be a cause of the different behavior.

Our findings show that MD simulations can explain the differences between HDT and the other two tyrosol-based metabolites observed with the ThT assay.

While HVA and TY compounds have a conserved hydroxyl group at the C4 position, HDT has an additional -OH group at C3 position which allow multiple interactions between GLU22 and ASP23 or between PHE19 and PHE20 at the same time (see Fig. 5 for snapshots of the interaction and Fig. 4A-B for the interaction energy profiles). We suggest it is the reason for a stronger binding respect HVA and TY. The difference in behavior between HVA and TY. Notably, it has been also demonstrated that a turn at positions 22 and 23 plays a critical role in driving the formation of toxic Aβ conformers [38–42]. We believe that the stronger binding of HDT to residues 22 and 23 may thus explain its specific effects on Aβ aggregation kinetics. The difference in behavior between HVA and TY, however, requires a more in-depth study.

4. Conclusions

We investigated the structure-activity relationship of three tyrosol-based ligands (HDT, TY, and HVA) in the self- assembly process of the amyloidogenic Aβ proteins. Interestingly, although the three metabolites present similar chemical structures, HDT is an effective inhibitor of Aβ aggregation, whereas TY and HVA catalyze Aβ aggregation. The presence of the additional hydroxyl group at the C-3 position in the HDT plays a crucial role in stabilizing ligand interactions with $A\beta_{1-40}$ by the formation of an H-bond network in the proximity of residue GLU 22. MD simulations suggest that the binding between HDT and $A\beta_{1-40}$ hinders the known amylogenic motif by stiffening the 16–19 region of the protein that has been reported to be significantly involved in the aggregation process. We hope that our results may inspire the future design of polyphenols with improved efficacy in inhibiting Aβ aggregation.

Author statement

V.R. synthesis, purification and analysis of HDT; S.G.-V. performed ThT assays; C.T. performed molecular dynamics simulations; R.B. synthesis of HDT; A.Z. chemical analysis of HDT, TY and HVA; F.L. performed and analyzed molecular dynamics simulations and wrote the paper; D.M. designed the research and wrote the paper; G.D.F. designed the research and wrote the paper.

Declaration of Competing Interest

The authors declare that they have no known competing financial interests or personal relationships that could have appeared to influence the work reported in this paper.

Acknowledgment

We acknowledge AIPRAS Onlus (Associazione Italiana per la Promozione delle Ricerche sull'Ambiente e la Saluta umana) for support of this investigation. F.L. wish to acknowledge CSC – IT Center for Science (Espoo, Finland) for computational resources. This work was partly financially supported by the Italian Ministry of University and Research (MIUR): PRIN 20157WZM8A. S.G.V. acknowledges the European Union Horizon 2020 research and innovation program for funding their Ph.D. fellowships under the Marie Sklodowska-Curie grant agreement INCIPIT n. 665403.

Appendix A. Supplementary data

Supplementary data to this article can be found online at https://doi.org/10.1016/j.bpc.2020.106434.

References

[1] Alzheimer"s Association, 2016 Alzheimer's disease facts and figures, Alzheimers Dement. 12 (2016) 459–509, https://doi.org/10.1016/j.jalz.2016.03.001.
[2] F. Mangialasche, A. Solomon, B. Winblad, P. Mecocci, M. Kivipelto, Alzheimer's disease: clinical trials and drug development, Lancet Neurol. 9 (2010) 702–716, https://doi.org/10.1016/S1474-4422(10)70119-8.
[3] G. Chen, T. Xu, Y. Yan, Y. Zhou, Y. Jiang, K. Melcher, H.E. Xu, Amyloid beta: structure, biology and structure-based therapeutic development, Acta Pharmacol. Sin. 38 (2017) 1205–1235, https://doi.org/10.1038/aps.2017.28.
[4] P.A. Galanakis, F.N. Bazoti, J. Bergquist, K. Markides, G.A. Spyroulias, A. Tsarbopoulos, Study of the interaction between the amyloid beta peptide (1-40) and antioxidant compounds by nuclear magnetic resonance spectroscopy, Biopolymers 96 (2011) 316–327, https://doi.org/10.1002/bip.21558.
[5] E. Evangelisti, R. Cascella, M. Becatti, G. Marrazza, C.M. Dobson, F. Chiti, M. Stefani, C. Cecchi, Binding affinity of amyloid oligomers to cellular membranes is a generic indicator of cellular dysfunction in protein misfolding diseases, Sci. Rep. 6 (2016) 32721, https://doi.org/10.1038/srep32721.
[6] M.F.M. Sciacca, S.A. Kotler, J.R. Brender, J. Chen, D. Lee, A. Ramamoorthy, Two-step mechanism of membrane disruption by Aβ through membrane fragmentation and pore formation, Biophys. J. 103 (2012) 702–710, https://doi.org/10.1016/j.bpj.2012.06.045.
[7] S.I.A. Cohen, S. Linse, L.M. Luheshi, E. Hellstrand, D.A. White, L. Rajah, D.E. Otzen, M. Vendruscolo, C.M. Dobson, T.P.J. Knowles, Proliferation of amyloid-β42 aggregates occurs through a secondary nucleation mechanism, Proc. Natl. Acad. Sci. U. S. A. 110 (2013) 9758–9763, https://doi.org/10.1073/pnas.1218402110.
[8] J. Mayes, C. Tinker-Mill, O. Kolosov, H. Zhang, B.J. Tabner, D. Allsop, β-Amyloid fibrils in alzheimer disease are not inert when bound to copper ions but can degrade hydrogen peroxide and generate reactive oxygen species, J. Biol. Chem. 289 (2014) 12052–12062, https://doi.org/10.1074/jbc.M113.525212.
[9] M.J. Guerrero-Muñoz, D.L. Castillo-Carranza, R. Kayed, Therapeutic approaches against common structural features of toxic oligomers shared by multiple amyloidogenic proteins, Biochem. Pharmacol. 88 (2014) 468–478, https://doi.org/10.1016/j.bcp.2013.12.023.
[10] R. Sperling, E. Mormino, K. Johnson, The evolution of preclinical Alzheimer's disease: implications for prevention trials, Neuron. 84 (2014) 608–622, https://doi.org/10.1016/j.neuron.2014.10.038.
[11] Q. Nie, X. Du, M. Geng, Small molecule inhibitors of amyloid β peptide aggregation as a potential therapeutic strategy for Alzheimer's disease, Acta Pharmacol. Sin. 32 (2011) 545–551, https://doi.org/10.1038/aps.2011.14.
[12] G. Di Fabio, V. Romanucci, C. Di Marino, L. De Napoli, A. Zarrelli, A rapid and simple chromatographic separation of Diastereomers of Silibinin and their oxidation to produce 2,3-Dehydrosilybin enantiomers in an optically pure form, Planta Med. 79 (2013) 1077–1080, https://doi.org/10.1055/s-0032-1328703.
[13] M.F.M. Sciacca, V. Romanucci, A. Zarrelli, I. Monaco, F. Lolicato, N. Spinella, C. Galati, G. Grasso, L. D'Urso, M. Romeo, L. Diomede, M. Salmona, C. Bongiorno, G. Di Fabio, C. La Rosa, D. Milardi, Inhibition of Aβ amyloid growth and toxicity by Silybins: the crucial role of stereochemistry, ACS Chem. Neurosci. 8 (2017) 1767–1778, https://doi.org/10.1021/acschemneuro.7b00110.
[14] I. Lejri, A. Agapouda, A. Grimm, A. Eckert, Mitochondria- and oxidative stress-targeting substances in cognitive decline-related disorders- and molecular mechanisms to clinical evidence, Oxidative Med. Cell. Longev. 2019 (2019), https://doi.org/10.1155/2019/9695412.
[15] A. Maruca, R. Catalano, D. Bagetta, F. Mesiti, F.A. Ambrosio, I. Romeo, F. Moraca, R. Rocca, F. Ortuso, A. Artese, G. Costa, S. Alcaro, A. Lupia, The Mediterranean diet as source of bioactive compounds with multi-targeting anti-cancer profile, Eur. J. Med. Chem. 181 (2019) 111579, https://doi.org/10.1016/j.ejmech.2019.111579.
[16] R. Bernini, N. Merendino, A. Romani, F. Velotti, Naturally occurring hydroxytyrosol: synthesis and anticancer potential, Curr. Med. Chem. 20 (2013) 655–670, https://doi.org/10.2174/092986713804999367.
[17] R. Bernini, I. Carastro, G. Palmini, A. Tanini, R. Zonefrati, P. Pinelli, M.L. Brandi, A. Romani, Lipophilization of hydroxytyrosol-enriched fractions from *Olea europaea* L. Byproducts and evaluation of the in vitro effects on a model of colorectal cancer cells, J. Agric. Food Chem. 65 (2017) 6506–6512, https://doi.org/10.1021/acs.jafc.6b05457.
[18] T. Hu, X.-W. He, J.-G. Jiang, X.-L. Xu, Hydroxytyrosol and its potential therapeutic effects, J. Agric. Food Chem. 62 (2014) 1449–1455, https://doi.org/10.1021/jf405820v.
[19] F. Casamenti, M. Stefani, Olive polyphenols: new promising agents to combat aging-associated neurodegeneration, Expert. Rev. Neurother. 17 (2017) 345–358, https://doi.org/10.1080/14737175.2017.1245617.
[20] F. Sarubbo, D. Moranta, G. Pani, Dietary polyphenols and neurogenesis: molecular interactions and implication for brain ageing and cognition, Neurosci. Biobehav. Rev. 90 (2018) 456–470, https://doi.org/10.1016/j.neubiorev.2018.05.011.
[21] M. Leri, A. Natalello, E. Bruzzone, M. Stefani, M. Bucciantini, Oleuropein aglycone and hydroxytyrosol interfere differently with toxic Aβ1-42 aggregation, Food Chem. Toxicol. 129 (2019) 1–12, https://doi.org/10.1016/j.fct.2019.04.015.
[22] C. St-Laurent-Thibault, M. Arseneault, F. Longpre, C. Ramassamy, Tyrosol and hydroxytyrosol two main components of olive oil, protect N2a cells against amyloid-β-induced toxicity. involvement of the NF-κβ signaling, Curr. Alzheimer Res. 8 (2011) 543–551, https://doi.org/10.2174/156720511796391845.
[23] M. Kurisu, Y. Miyamae, K. Murakami, J. Han, H. Isoda, K. Irie, H. Shigemori, Inhibition of amyloid β aggregation by acteoside, a phenylethanoid glycoside, Biosci. Biotechnol. Biochem. 77 (2013) 1329–1332, https://doi.org/10.1271/bbb.130101.
[24] K.J. Korshavn, M. Jang, Y.J. Kwak, A. Kochi, S. Vertuani, A. Bhunia, S. Manfredini, A. Ramamoorthy, M.H. Lim, Reactivity of metal-free and metal-associated amyloid-β with glycosylated polyphenols and their esterified derivatives, Sci. Rep. 5 (2015) 17842, https://doi.org/10.1038/srep17842.
[25] R. Bernini, E. Mincione, M. Barontini, F. Crisante, Convenient synthesis of hydroxytyrosol and its lipophilic derivatives from tyrosol or homovanillyl alcohol, J. Agric. Food Chem. 56 (2008) 8897–8904, https://doi.org/10.1021/jf801558z.
[26] K. Gade Malmos, L.M. Blancas-Mejia, B. Weber, J. Buchner, M. Ramirez-Alvarado, H. Naiki, D. Otzen, ThT 101: a primer on the use of thioflavin T to investigate amyloid formation, Amyloid 24 (2017) 1–16, https://doi.org/10.1080/13506129.2017.1304905.
[27] M.J. Abraham, T. Murtola, R. Schulz, S. Páll, J.C. Smith, B. Hess, E. Lindahl, GROMACS: high performance molecular simulations through multi-level parallelism from laptops to supercomputers, SoftwareX 1–2 (2015) 19–25.
[28] S. Vivekanandan, J.R. Brender, S.Y. Lee, A. Ramamoorthy, A partially folded structure of amyloid-beta(1-40) in an aqueous environment, Biochem. Biophys. Res. Commun. 411 (2011) 312–316, https://doi.org/10.1016/j.bbrc.2011.06.133.
[29] J. Huang, S. Rauscher, G. Nawrocki, T. Ran, M. Feig, B.L. de Groot, H. Grubmüller, A.D. MacKerell, CHARMM36m: an improved force field for folded and intrinsically disordered proteins, Nat. Methods 14 (2017) 71–73.
[30] T. Darden, D. York, L. Pedersen, Particle mesh Ewald: an $N \cdot \log(N)$ method for Ewald sums in large systems, J. Chem. Phys. 98 (1993) 10089–10092, https://doi.org/10.1063/1.464397.
[31] S. Nosé, M.L. Klein, Constant pressure molecular dynamics for molecular systems, Mol. Phys. 50 (1983) 1055–1076, https://doi.org/10.1080/00268978300102851.
[32] Polymorphic transitions in single crystals: a new molecular dynamics method, J. Appl. Phys. 52 (1981) 7182–7190, https://doi.org/10.1063/1.328693.
[33] L.M. Young, J.C. Saunders, R.A. Mahood, C.H. Revill, R.J. Foster, L.H. Tu, D.P. Raleigh, S.E. Radford, A.E. Ashcroft, Screening and classifying small-molecule inhibitors of amyloid formation using ion mobility spectrometry-mass spectrometry, Nat. Chem. 7 (2015) 73–81, https://doi.org/10.1038/nchem.2129.
[34] A.J. Queimada, F.L. Mota, S.P. Pinho, E.A. Macedo, Solubilities of biologically active phenolic compounds: measurements and modeling, J. Phys. Chem. B 113 (2009) 3469–3476, https://doi.org/10.1021/jp808683y.
[35] A.T. Petkova, Y. Ishii, J.J. Balbach, O.N. Antzutkin, R.D. Leapman, F. Delaglio, R. Tycko, A structural model for Alzheimer's -amyloid fibrils based on experimental constraints from solid state NMR, Proc. Natl. Acad. Sci. 99 (2002) 16742–16747, https://doi.org/10.1073/pnas.262663499.
[36] J.S. Pedersen, G. Christensen, D.E. Otzen, Modulation of S6 fibrillation by unfolding rates and gatekeeper residues, J. Mol. Biol. 341 (2004) 575–588, https://doi.org/10.1016/j.jmb.2004.06.020.
[37] M. Valerio, A. Colosimo, F. Conti, A. Giuliani, A. Grottesi, C. Manetti, J.P. Zbilut, Early events in protein aggregation: molecular flexibility and hydrophobicity/charge interaction in amyloid peptides as studied by molecular dynamics simulations, Proteins Struct. Funct. Bioinforma. 58 (2004) 110–118, https://doi.org/10.1002/prot.20306.
[38] S.T. Mutter, M. Turner, R.J. Deeth, J.A. Platts, Molecular dynamics simulations of copper binding to amyloid-β Glu22 mutants, Heliyon 6 (2020) e03071, , https://doi.org/10.1016/j.heliyon.2019.e03071.
[39] S. Shuaib, B. Goyal, Scrutiny of the mechanism of small molecule inhibitor preventing conformational transition of amyloid-β42 monomer: insights from molecular dynamics simulations, J. Biomol. Struct. Dyn. 36 (2018) 663–678, https://doi.org/10.1080/07391102.2017.1291363.
[40] B.R. Sahoo, T. Genjo, T.W. Nakayama, A.K. Stoddard, T. Ando, K. Yasuhara, C.A. Fierke, A. Ramamoorthy, A cationic polymethacrylate-copolymer acts as an agonist for β-amyloid and an antagonist for amylin fibrillation, Chem. Sci. 10 (2019) 3976–3986, https://doi.org/10.1039/c8sc05771k.
[41] D. Pramanik, S.G. Dey, Active site environment of heme-bound amyloid β peptide associated with Alzheimers disease, J. Am. Chem. Soc. 133 (2011) 81–87, https://doi.org/10.1021/ja1084578.
[42] B. Mehrazma, S. Opare, A. Petoyan, A. Rauk, D-amino acid pseudopeptides as potential amyloid-beta aggregation inhibitors, Molecules 23 (2018), https://doi.org/10.3390/molecules23092387.